Comb Polymers Prepared by ATRP from Hydroxypropyl Cellulose

Emma Östmark,[†] Simon Harrisson,[‡,§] Karen L. Wooley,[‡] and Eva E. Malmström*[,†]

Royal Institute of Technology, KTH Fibre and Polymer Technology, Teknikringen 56-58, 100 44 Stockholm, Sweden, and Center for Materials Innovation and Department of Chemistry, Washington University in Saint Louis, One Brookings Drive, Saint Louis, Missouri 63130

Received October 31, 2006; Revised Manuscript Received December 27, 2006

Hydroxypropyl cellulose (HPC) was used as a core molecule for controlled grafting of monomers by ATRP, the aim being to produce densely grafted comb polymers. HPC was either allowed to react with an ATRP initiator or the first generation initiator-functionalized 2,2-bis(methylol)propionic acid dendron to create macroinitiators having high degrees of functionality. The macroinitiators were then "grafted from" using ATRP of methyl methacrylate (MMA) or hexadecyl methacrylate. Block copolymers were obtained by chain extending PMMA-grafted HPCs via the ATRP of *tert*-butyl acrylate. Subsequent selective acidolysis of the *tert*-butyl ester moieties was performed to form a block of poly(acrylic acid) resulting in amphiphilic block copolymer grafts. The graft copolymers were characterized by ^{1}H NMR and FT−IR spectroscopies, DSC, TGA, rheological measurements, DLS, and tapping mode AFM on samples spin coated upon mica. It was found that the comb (co)polymers were in the nanometer size range and that the dendronization had an interesting effect on the rheological properties.

Introduction

The synthesis of polymers with well-defined architectures has been a focus of many research activities since the introduction of the "living"/controlled polymerization techniques. Complex architectures, such as star and comb polymers with a high grafting density, were not realistic synthetic goals until techniques providing more control were established; these techniques have since had a tremendous impact on the development of novel pre-designed materials. For instance, dendronized polymers are one of the new architectures that have gained increasing attention during the latest years.[1−4] This subclass of comb polymers was first proposed in a patent by Tomalia in 1987[5] and was thereafter accomplished by Hawker and Fréchet using Fréchet-type dendrons in 1992.[6] These molecules are interesting because of their unique physical properties that arise from the steric crowding at higher generations, which results in an extended rod-shaped polymer.[7] Several appealing applications for dendronized polymers have been suggested based upon their size and versatile post-functionalization possibilities.

Cellulose is an interesting natural substrate for grafting because of its combination of reactivity, mechanical strength, high abundance, low cost, and renewability. The grafting of polymers from cellulose using conventional polymerization techniques was widely investigated during the last century, and the resulting copolymers normally offer sufficient properties for less sophisticated industrial applications. However, more specific application areas require denser, better-defined grafts of predetermined degrees of polymerization (DP), which can only be obtained by the use of "living"/controlled polymerization techniques. In addition, the living character of the polymerization permits the creation of block copolymers and/or sequential post-modification. For instance, cellulose, in the form of filter paper, has been used as a substrate for graft polymerization by ATRP of MA,[8] MA-*b*-HEMA,[9] and DMAEMA to create antibacterial surfaces.[10] Other solid cellulose substrates, such as cellulose powders,[11] microcrystalline cellulose, Lyocell fibers, and dialysis tubing, have also recently been employed in grafting using ATRP.[12] Comb polymers, grafted from dissolved cellulose molecules, have been synthesized by nitroxide mediated polymerization of styrene from hydroxypropyl cellulose using Barton ester intermediates;[13] by ring-opening polymerization of ϵ-caprolactone from hydroxypropyl cellulose;[14,15] by ATRP of methyl methacrylate (MMA), styrene, and *n*-butyl acrylate from cellulose diacetate;[16,17] by ATRP of MMA or styrene from hydroxyethyl cellulose;[18] and by RAFT polymerization of styrene employing hydroxypropyl cellulose.[19,20]

When ATRP is performed from a multifunctional initiator, radical−radical coupling of the propagating chains is likely to occur because of the high local concentration of radicals, which results in a gel. Gelation can be prevented through various methods, such as the addition of a deactivator[21] or by diluting the reaction mixture. The concentration of radicals will change with the monomer conversion since unreacted monomer has a diluting effect on the reaction mixture.[22,23]

Dendronized polymers containing the 2,2-bis(methylol)-propionic acid (bis-MPA) unit have been widely studied by our group[3,24,25] and others recently,[26−31] and promising applications have been suggested. To the authors' knowledge, however, dendronization of cellulose has not been conducted using the bis-MPA unit but through regioselective dendronization with focal isocyanate-functionalized dendrons[32,33] and attachment of a first generation trifunctional aminoamide to carboxymethyl cellulose.[34] However, the dendron density could be increased by using a cellulose derivative with more available groups for dendronization.

In the present paper, hydroxypropyl cellulose (HPC) is investigated as a backbone for "grafting from" polymerization

* Corresponding author. Tel.: +46 8 790 82 73. Fax: +46 8 790 82 83. E-mail: mave@polymer.kth.se.

† Royal Institute of Technology.

‡ Washington University in Saint Louis.

§ Current address: CSIRO Molecular and Health Technologies, Bayview Ave, Clayton VIC 3169, Australia.

10.1021/bm061043w CCC: $37.00
Published on Web 03/17/2007

under ATRP conditions to produce comb polymers. Moreover, dendronization of the hydroxypropyl cellulose using bis-MPA dendrons and subsequent ATRP grafting from the surface of the dendronized polymer was studied. The advantage of using HPC is the available hydroxyl groups, which show high reactivity with bis-MPA derivatives combined with the improved solubility HPC exhibits as compared to native cellulose. Furthermore, bis-MPA and HPC are both biocompatible, which could make these dendronized polymers promising candidates for biomedical applications.

Experimental Procedures

Materials. Hydroxypropyl cellulose (M_n = 10 000 g mol^{-1} and M_w = 80 000 g mol^{-1} according to manufacturer; M_n = 25 200 g mol^{-1} and M_w = 63 600 g mol^{-1} obtained using SEC with THF as mobile phase and molar substitution of propoxy groups (MS_{HP}) of 2.9 determined using ^{1}H NMR), *N*,*N*′,*N*″,*N*‴-pentamethyldiethylenetriamine (PMDETA) (99%), and 4-(dimethylamino)pyridine (DMAP) (99%) were purchased from Aldrich and used as received. 2-Bromoisobutyryl bromide, 2-bromoisobutyric acid, copper(I)bromide, copper(II)bromide, *N*,*N*′-dicyclohexylcarbodiimide (99%), trifluoroacetic acid (99%), and oxalyl chloride (98%) were obtained from Acros Organics. 2,2-Bis(methylol)propionic acid (bis-MPA) was kindly supplied by Perstorp AB. Benzyl-2,2-bis(methylol)propionate and 3-(2-bromo-2-methylpropanoyloxy)-2-((2-bromo-2-methylpropanoyloxy)-methyl)-2-methylpropanoic acid were prepared according to methods described in the literature.[35,36] All monomers, MMA, *tert*-butyl acrylate (*t*-BA), and hexadecyl methacrylate (HDMA), were purified by being passed through a column of activated neutral alumina (Merck). All other chemicals were used as received.

Instrumentation. Nuclear Magnetic Resonance. ^{1}H− and ^{13}C NMR spectra were recorded on a Bruker AM 400 or on a Bruker Avance 400 MHz NMR instrument using $CDCl_3$ or DMSO-d_6. The solvent signals were used as internal standards.

Fourier Transform Infrared Spectroscopy. The absorption spectra were collected by employing a Perkin-Elmer spectrum 2000 FT−IR equipped with a MKII Golden Gate, single reflection ATR system from Specac Ltd. The ATR crystal was a MKII heated diamond 45° ATR top plate. Sixteen scans were recorded for each spectrum.

Size Exclusion Chromatography. SEC using THF (1.0 mL min^{-1}) as the mobile phase was performed at 35 °C using a Viscotek TDA model 301 equipped with two GMH_{HR}-M columns with TSK gel (mixed bed, M_W resolving range: 300−100 000) from Tosoh Biosep, a VE 5200 GPC autosampler, a VE 1121 GPC solvent pump, and a VE 5710 GPC degasser (all from Viscotek Corp.). A calibration method was created using broad and narrow linear polystyrene standards. Corrections for the flow rate fluctuations were made using toluene as an internal standard. Viscotek OmniSEC version 4.0 software was used to process data.

Dynamic Light Scattering (DLS). Particle size distributions were determined on a Brookhaven Instruments Co. DLS system, consisting of a model BI-9000T digital goniometer, a model EMI-9865 photomultiplier, and a model 95−2 Ar laser (Lexel Corp.) operating at 514.5 nm. Measurements were made at 20 ± 1 °C. Prior to analysis, solutions were made in toluene, filtered through a 0.22 μm filter, and centrifuged in a model 5414 microfuge (Brinkman Instrument Co.) for 4 min to remove dust particles. Scattered light was collected at a fixed angle of 90°. The digital correlator was operated with 522 channels, an initial delay of 1.0 μs, a final delay of 10 ms, and a duration time of 5 or 10 min. A photomultiplier aperture of 200 μm was used. Only measurements for which the measured and calculated baselines of the intensity autocorrelation function agreed to within ± 0.1% were used to calculate nanoparticle diameter distributions. All determinations were made in triplicate.

The calculations of the nanoparticle diameter distributions were performed using the ISDA software package (Brookhaven Instruments Co.).

Atomic Force Microscopy. AFM samples were prepared through spin casting (3500 rpm, 90 s) solutions of polymer samples in toluene (0.01−1.0 mg mL^{-1}) (except for native HPC, dissolved in water) onto freshly cleaved mica. AFM was performed using Nanoscope III-a system (Digital Instruments) equipped with a *J*-type vertically engaged piezoelectric scanner operating in tapping mode in air. Silicon AFM probes from Nanosensors were used throughout the study (l = 125 μm, force constant ≈42 N/m, and resonance frequency ≈320 kHz).

Thermogravimetric Analysis (TGA). TGA was performed on a Mettler Toledo TGA/SDTA851 TGA module and evaluated using STAR^e software, version 8.10. Heating was performed at 10 °C min^{-1} with an O_2 flow of 50 mL min^{-1}.

Differential Scanning Calorimetry. DSC thermograms were collected using a Mettler Toledo DSC820 using a heating/cooling rate of 10 °C min^{-1} under N_2 atmosphere. STARe software, version 8.10, was used to evaluate data.

Rheological Measurements. Rheological properties of the polymers were investigated using an ARES Rheometer (TA Instruments). The tests were performed in dynamic mode using a parallel plate configuration. The plates had a diameter of 8 mm. The sample was first melted between the plates at 160 °C, to ensure good contact between the plates and a uniform thickness. Dynamic frequency sweep tests were performed between 1 and 10^2 rad s^{-1} at a temperature range of 125−150 °C, at intervals of 5 °C with a strain of approximately 0.5%. Master curves, showing the frequency dependence of the shear modulii G' and G'' or complex viscosities *Eta**, with T_{ref} = 135 °C, over the frequency range of ca. 10^{-2} to 10^4 rad s^{-1} were created.

Synthesis. Synthesis of 2-Bromoisobutyryl Anhydride. 2-Bromoisobutyric acid (10.0 g, 59.9 mmol) was dissolved in CH_2Cl_2 (75 mL). *N*,*N*′-Dicyclohexylcarbodiimide (6.80 g, 32.9 mmol) was added, and the milky mixture was stirred at ambient temperature overnight. The precipitate was filtered off, and the filtrate was concentrated through rotary evaporation and precipitated into dry ice cold *n*-heptane. The residue was filtered, washed with cold *n*-heptane, and dried under reduced pressure. The resulting white solid was afforded in 50.4% yield. ^{1}H NMR ($CDCl_3$): δ 1.99 (s, 12H, CH_3) ppm. ^{13}C NMR ($CDCl_3$): δ 30.12, 55.10, 165.84 ppm.

Synthesis of Hydroxypropyl Cellulose Macroinitiator (HPC−I). Hydroxypropyl cellulose (HPC; 0.50 g) was dissolved in *N*,*N*-dimethylformamide (DMF; 50 mL). 4-(Dimethylamino)pyridine (DMAP; 0.19 g, 1.6 mmol) and pyridine (4.6 mL) were added and carefully dissolved under stirring. 2-Bromoisobutyryl anhydride (5.00 g, 15.8 mmol) was then added to the solution, and the reaction was allowed to proceed with stirring for 12 h at room temperature. The reaction was terminated by quenching the anhydride with the addition of water (∼10 mL), which resulted in the precipitation of the product as a sticky white solid. The mixture was vigorously stirred during 48 h, the solvents were filtered off, and the precipitate was dried under vacuum. The product was dissolved in a small volume of CH_2Cl_2 and precipitated in dry ice cold *n*-heptane (500 mL). The product was filtered, washed with cold *n*-heptane, and dried under reduced pressure yielding a brown polymer. Elemental Anal.: C: 44.0%, O: 23.4%, H: 6.3%, Br: 27.2%. ^{1}H NMR ($CDCl_3$): δ 1.12 (br), 1.25 (br), 1.91 (s), 2.90−4.40 (br), 3.57 (value of sharpest peak inside broad peak), 5.03 (br) ppm. ^{13}C NMR ($CDCl_3$): δ 16.46−17.74, 30.93, 56.30, 71.50, 75.25, 170.81−171.14 ppm.

Synthesis of First Generation Dendronized Hydroxypropyl Cellulose Macroinitiator (HPC-G1-I). (A) Synthesis of 3-(2-Bromo-2-methylpropanoyloxy)-2-((2-bromo-2-methylpropanoyl-oxy)methyl)-2-methylpropanoic Acid Chloride (1). Oxalyl chloride (2.90 g, 23.1 mmol) was added dropwise to a solution of 3-(2-bromo-2-methylpropanoyloxy)-2-((2-bromo-2-methylpropanoyloxy)methyl)-2-methylpropanoic acid (5.00 g, 11.6 mmol) and 3 drops of DMF in CH_2Cl_2 (100 mL). The reaction was allowed to proceed at room temperature while stirring for 4 h. The solvent and excess of oxalyl chloride were removed on the rotary evaporator. Any residual oxalyl chloride was removed through stripping of the product with small portions of CH_2Cl_2. The

product was dried under vacuum at 50 °C for 24 h, yielding a yellow oil in 98%. ^{1}H NMR ($CDCl_3$): δ 1.42 (s, 3H, -CH_3) 1.86 (s, 12H, -C(Br)(CH_3)$_2$), 4.36−4.37 (br, 4H, -CH_2-) ppm. ^{13}C NMR ($CDCl_3$): δ 17.89, 30.54, 54.94, 56.22, 65.79, 170.68, 174.87 ppm.

(B) Synthesis of Macroinitiator. To a solution of hydroxypropyl cellulose (0.25 g) in DMF (25 mL) were added DMAP (0.15 g, 1.2 mmol) and triethylamine (TEA; 1.20 g, 11.9 mmol). 3-(2-Bromo-2-methylpropanoyloxy)-2-((2-bromo-2-methylpropanoyloxy)methyl)-2-methylpropanoic acid chloride (3.7 g, 7.9 mmol) was added, and a salt immediately precipitated. The reaction was allowed to proceed while stirring for 12 h at room temperature. The reaction was terminated by the addition of water (~5 mL), which resulted in the precipitation of the product as a sticky yellow solid. The mixture was vigorously stirred for 48 h, the solvents were filtered off, and the precipitate was dried under vacuum. The product was dissolved in a small volume of CH_2Cl_2 and precipitated in dry ice cold *n*-heptane (300 mL). The product was filtered, washed with cold *n*-heptane, and dried under reduced pressure yielding a slightly brownish polymer. Elemental Anal.: C: 46.7%, O: 26.9%, H: 6.4%, Br: 20.3%. ^{1}H NMR ($CDCl_3$): δ 1.12 (br), 1.25 (br), 1.32 (br), 1.75 (br), 1.91 (s), 2.90−4.20 (br), 3.55 (value of sharpest peak inside broad peak), 4.31 (br), 4.38 (br), 5.06 (br) ppm. ^{13}C NMR ($CDCl_3$): δ 16.81−17.66, 18.11, 29.82, 30.82, 46.69, 55.57, 64.56, 66.29, 170.80−170.99, 171.59−171.83 ppm.

General Procedure for Polymerization from the Macroinitiators. HPC−I (0.050 g, 0.17 mmol of Br) was added to a flask containing a reaction mixture of MMA (6.0 g, 60 mmol), PMDETA (104 mg, 0.60 mmol), and toluene (6.0 g, 50 wt %). When then initiator was completely dissolved, Cu(I)Br (69 mg, 0.48 mmol) and Cu(II)Br_2 (27 mg, 0.12 mmol) were added, and the flask was sealed with a rubber septum. The flask was evacuated and back-filled with Ar gas 3 times and thereafter immersed into an oil bath set to 80 °C. When the viscosity of the reaction mixture had increased significantly (19 h), an aliquot was withdrawn with a syringe (for conversion measurements with ^{1}H NMR), and the reaction was terminated through withdrawal from the oil bath, air exposure, and dilution with THF. The solution was then passed through a short column containing aluminum oxide (neutral) to remove the copper complex, precipitated into dry ice cold methanol, filtered, washed, and dried under vacuum. ^{1}H NMR ($CDCl_3$): δ 0.85 (s, -C(C*H*$_3$)(COOCH$_3$)), 1.02 (s, -C(C*H*$_3$)(COOCH$_3$)), 1.81−2.07 (-CH_2-, (br, polymer backbone)), 3.60 ppm (s, -C(CH$_3$)(COOC*H*$_3$)). FT−IR: 748, 841, 966, 988, 1064, 1145, 1191, 1240, 1268, 1388, 1435, 1479, 1724, 2950, 2995 cm^{-1}.

Preparation of HPC-*graft*-PMMA-*block*-PtBA. HPC-*graft*-PMMA (0.100 g) was dissolved in a flask containing *t*-BA (6.0 g, 47 mmol), PMDETA (81 mg, 0.47 mmol), and toluene (6.0 g, 50 wt %). Cu(I)Br (54 mg, 0.38 mmol) and Cu(II)Br_2 (21 mg, 94 μmol) were added, and the flask was sealed with a rubber septum. The flask was evacuated and back-filled with Ar gas 3 times and then immersed into an oil bath set to 70 °C. After 22 h, the reaction was terminated, and the polymer was isolated as stated earlier (yield: 0.170 g). The weight of the polymer had increased by 70 mg. ^{1}H NMR ($CDCl_3$): 0.84 (s, -C(C*H*$_3$)(COOCH$_3$)), 1.02 (s, -C(C*H*$_3$)(COOCH$_3$), 1.26−1.90 (-CH_2-br, polymer backbones), 1.44 (s, -CH_2(CHOOC(C*H*$_3$)$_3$)), 2.15−2.30 (br, -CH_2(C*H*OOC(CH$_3$)$_3$)), 3.60 ppm (s, -C(CH$_3$)(COOC*H*$_3$)). FT−IR: 751, 846, 991, 1060, 1066, 1143, 1257, 1366, 1392, 1455, 1723, 2854, 2922, 2947 cm^{-1}.

Acidolysis of the *tert*-Butyl Group for the Preparation of HPC-*graft*-PMMA-*block*-PAA. HPC-*graft*-PMMA-*block*-PtBA (0.050 g) was allowed to dissolve in a round-bottomed flask containing THF (~2 mL, HPLC grade), and then an excess of trifluoroacetic acid (TFA; 0.68 g, 0.44 mL) was added. The reaction was stirred at ambient temperature for 48 h, whereafter the THF and TFA were removed via rotary evaporation. The resulting polymer was stirred in a THF/water mixture for 48 h to remove any anhydride formed. Thereafter, the solvents were evaporated, and the polymer was dried at 50 °C under vacuum yielding a slightly green polymer. FT−IR: 699, 724, 750, 797, 844, 922, 963, 1035, 1063, 1144, 1191, 1448, 1702, 1720, 1786, 2856, 2926, 2952, 3160 cm^{-1}.

Scheme 1. Preparation of Macroinitiators, HPC-I and HPC-G1-I (Idealized Cartoons), through Esterification Using the Anhydride of the Initiator and Hydroxypropyl Cellulose (HPC; Left) and Esterification Using the Acid Chloride of the First Generation bis-MPA Dendron Initiator (Right)

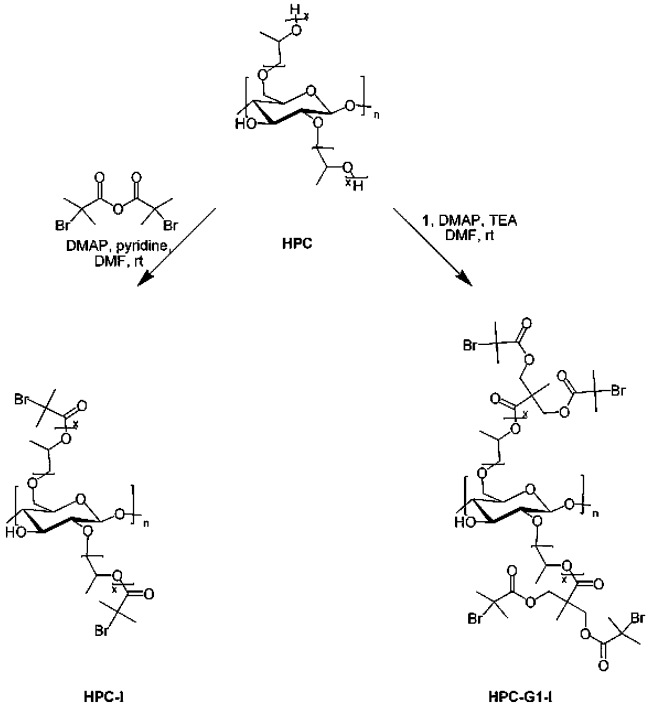

Results and Discussion

Synthesis of Macroinitiators. HPC was chosen as a core backbone structure from which copper(I) mediated atom transfer radical polymerization (ATRP) was performed because it is a renewable resource combining high molecular weight, reactivity, and acceptable solubility in organic solvents. One significant drawback with using HPC is, however, the difficult characterization and, in comparison to many synthetic polymers, limited solubility. The molar substitution (MS), defined as the number of propoxy groups per anhydroglucose unit, was determined to be 2.9 using ^{1}H NMR at 95 °C of HPC dissolved in DMSO-d_6. The hydroxyl groups of HPC were allowed to react with the anhydride of 2-bromoisobutyric acid, yielding a multifunctional macroinitiator, HPC−I, suitable for the initiation of ATRP, containing a cellulose backbone (Scheme 1).

The substitution of the hydroxyl groups was monitored with FTIR and NMR spectroscopies, SEC, and elemental analysis. FTIR spectroscopy was especially convenient to monitor the formation of HPC−I (Figure 1). As can be seen, the conversion of HPC to HPC−I was successful and nearly quantitative since the broad peak at 3400 cm^{-1} originating from the hydroxyl groups in native HPC disappeared almost completely. In addition, the HPC−I spectrum shows an absorbance peak at 1730 cm^{-1}, not present in native HPC, which originates from the carbonyl groups of the newly formed α-bromoesters.

In the ^{1}H NMR spectrum of HPC−I, the appearance of a singlet resonating at 1.91 ppm, originating from the protons in the methyl groups of the initiating moieties, further confirmed the esterification. Moreover, the appearance of an additional peak at 1.25 ppm in the NMR spectrum of HPC−I is an effect of the reaction, which causes the resonances of the methyl

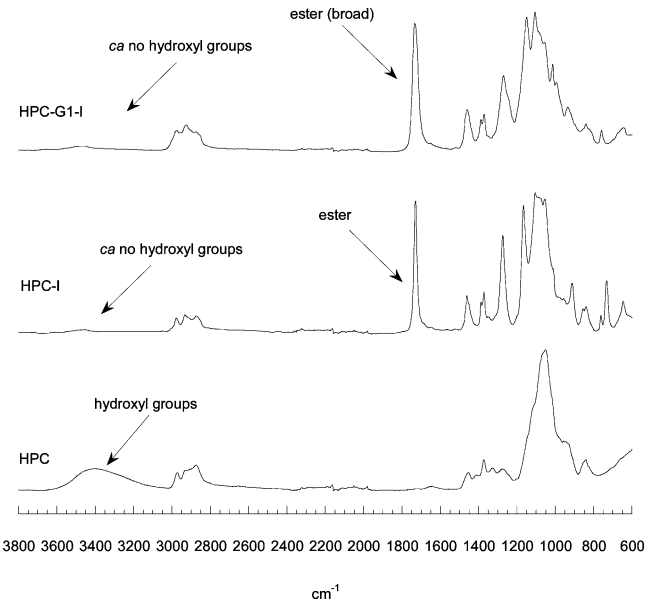

Figure 1. FTIR of native HPC, the macroinitiator HPC-I, and the first generation dendronized macroinitiator HPC-G1-I.

Table 1. Molecular Weights and Polydispersities Obtained with SEC in THF of HPC and Macroinitiators HPC-I and HPC-G1-I

sample	M_n (g mol)	M_w (g mol)	PDI
HPC	25 200	63 600	2.5
HPC-I	29 900	63 900	2.1
HPC-G1-I	34 400	66 300	1.9

groups on the hydroxypropyl side chains of HPC, which are closest to the initiator moieties, to shift downfield from their original position at 1.12 ppm.[15] In addition, there is a peak at 5.03 ppm in the HPC−I spectrum, which is not present in the spectrum of HPC. Two-dimensional ^{1}H NMR correlation spectroscopy studies of HPC derivatives have previously shown that this resonance is a signature of the methine proton that is coupled to the methyl at 1.25 ppm,[15] implying that the peak observed at 5.03 ppm is due to the methine protons closest to the initiator moieties. In the ^{13}C NMR spectroscopy studies, the amount of sample needed to obtain a good spectrum was found to be relatively high, and although the sample signal was acquired for a long time, it was not possible to detect all the resonance frequencies of HPC. However, for HPC−I, peaks at 170−171 ppm could be seen clearly, which are assigned to the ester carbonyl. An intense peak at 30.93 ppm, arising from the methyl groups alpha to the bromines, could also be observed in the ^{13}C NMR spectrum. The HPC and the initiator-modified HPCs (HPC−I and HPC-G1-I) were characterized by SEC in THF. As can be seen in Table 1, there was a significant increase in the molecular weight after the initiating groups were attached. The M_n increased from 25 200 g mol^{-1} (HPC) to 29 900 g mol^{-1} (HPC−I), which again confirmed the occurrence of the reaction.

The bromine content of HPC−I was determined to be 27.2 wt % by elemental analysis. This result further confirmed the attachment of the bromine containing initiating groups. The total degree of substitution (DS) for HPC−I was calculated, using the bromine content obtained from elemental analysis, to be 2.26, which means that 2.26 of the three hydroxyl groups per anhydroglucose unit have formed an ester with the initiating moiety. The first generation dendronized macroinitiator (HPC-G1-I) was synthesized by reacting the acid chloride of the first generation initiator-modified 2,2-bis(methylol)propionic acid (bis-MPA) with HPC (Scheme 1). bis-MPA was first converted into the corresponding 2-bromoisobutyrate ester through reaction with 2-bromoisobutyryl bromide according to Hedrick et al.[36] Thereafter, the reactivity of the acid group was augmented through conversion to the corresponding acid chloride (Scheme 2), which was allowed to react with the hydroxyl groups of HPC.

As in the FTIR spectrum of HPC−I, the attachment of initiator-modified dendrons to HPC resulted in a large decrease in the absorbance of the hydroxyl groups at 3400 cm^{-1} (Figure 1). A carbonyl peak at 1733 cm^{-1} was observed, which was somewhat broader than that of HPC−I, probably due to the two different esters in the resulting molecule, one arising from the ester attached to HPC and one from the bis-MPA ester. The resonance from the methyl groups of the initiating moieties at 1.91 ppm was clearly seen in the ^{1}H NMR spectrum of HPC-G1-I. As for HPC−I, the appearance of a new peak at 1.25 ppm in the ^{1}H NMR spectrum of HPC-G1-I could be observed, corresponding to the methyl groups on HPC closest to the initiating moieties. At 5.06 ppm, the methine proton resonance was observed. In addition to the peaks observed in both HPC−I and HPC-G1-I, the latter exhibited some peaks associated with the bis-MPA unit. The peak at 1.32 ppm corresponds to the methyl proton, and the somewhat broad double peaks at 4.31 and 4.38 ppm are due to the methylene protons of the bis-MPA unit. As for HPC−I, it was difficult to obtain a well-defined ^{13}C NMR spectrum of HPC-G1-I. However, ester carbonyl resonances at 170−172 ppm, corresponding to both the formed ester links to HPC and the pre-existing esters of the initiator moiety, as well as a peak at 30.82 ppm from the methyl groups alpha to the bromine in the initiator could easily be observed. Faint resonances could be seen at 18.11, 46.69, and 66.29 ppm corresponding to the methyl, quaternary, and methylene carbons, respectively, of the bis-MPA unit. Through SEC analysis (Table 1), it was confirmed that the molecular weight of HPC-G1-I, M_n = 34 400 g mol^{-1}, was higher than that of HPC, indicating a successful reaction. The molecular weight averages of HPC-G1-I are also generally higher than those of HPC−I, which implies that higher molecular weight molecules were attached to HPC. Elemental analysis of HPC-G1-I showed a bromine content of 20.3 wt %. The DS for HPC-G1-I was calculated as for HPC−I to be 0.88, meaning that the average number of initiating sites per anhydroglucose unit is 1.76 since each attached group contributed with two initiating sites. The number of initiating sites is thus higher for HPC−I than for HPC-G1-I. The lower degree of substitution of the first generation initiator as compared to the initiating group in HPC−I might be due to crowding.

ATRP from the Macroinitiators. The macroinitiators were used for polymerizations of methyl methacrylate, hexadecyl methacrylate, and *tert*-butyl acrylate under ATRP conditions. The macroinitiator was added to a reaction mixture containing monomer, solvent, and ligand and was allowed to dissolve completely before the reaction was started through the addition of copper salts and degassing. Since the macroinitiators were of quite high molecular weight, it was important that they were allowed to dissolve thoroughly before the reaction was initiated, as polymerization from an undissolved macroinitiator would be expected to lead to uneven grafting of HPC.

HPC−I was used to initiate the polymerization of several monomers to produce the resulting graft copolymers having, for example, PMMA chains extending from a cellulosic backbone as shown in Scheme 3. Different reaction conditions were employed to obtain well-defined, soluble polymers (Table 2).

Scheme 2. Preparation of the Acid Chloride of the First Generation Dendron bis-MPA Initiator[a]

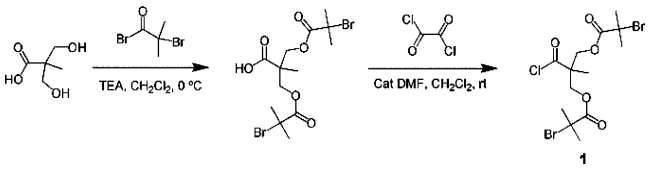

[a] bis-MPA unit is first functionalized with an ATRP initiator, and thereafter, the reactivity is enhanced through converting it to the corresponding acid chloride.

Scheme 3. Polymerization of MMA, Initiated by the Macrointiator HPC-I, under ATRP Conditions, Followed by Chain Extension Using *tert*-BA to Form a Second Block, Initiated by HPC-PMMA

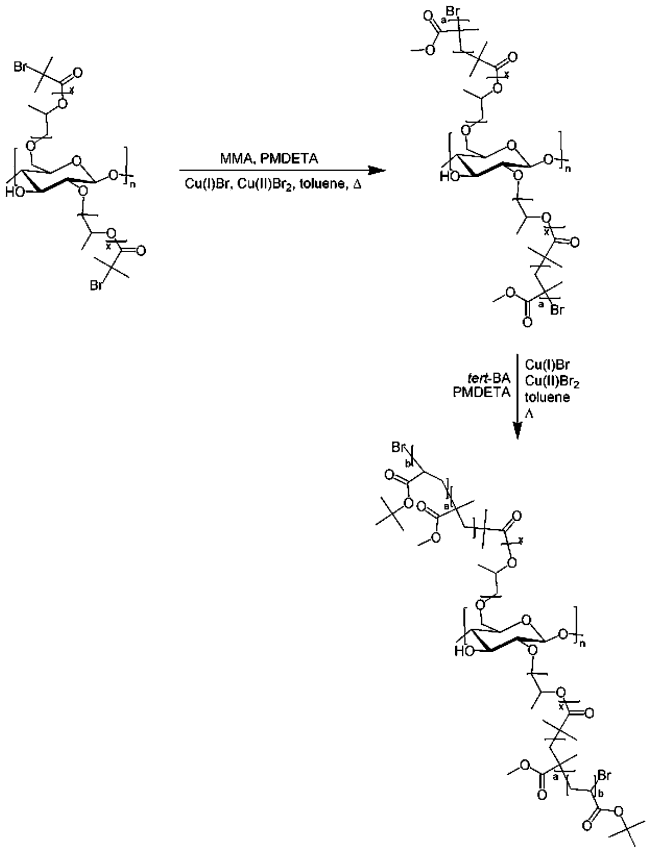

As can be seen in Table 2, dilution of the samples with at least 50 wt % solvent, in this case toluene, was found to be important to prevent gelation during ATRP. Because of the high number of initiating sites on the macroinitiators, dilute reaction conditions were required to maintain a low concentration of radicals and a controlled polymerization, with minimal intermolecular coupling. The addition of a deactivator in the form of $Cu(II)Br_2$ (at least 1:4 Cu(II)/Cu(I)) was essential to obtain a reasonably controlled polymerization. This results in a decreased concentration of propagating radicals and thus a slower rate of polymerization.[21] The radical concentration can also be reduced by lowering the reaction temperature: this technique was also utilized to optimize the polymerizations.

SEC analysis was found to be of little use in the characterization of the comb polymers. During sample preparation, the dilute polymer solutions were not all easily filtered through 0.45 μm filters, which may be due to their high molecular weight, aggregation, or comb−comb coupling during polymerization. Just a small portion of comb−comb coupling will result in molecules with extremely high molecular weights, which could clog the columns and render SEC analysis unreliable. However, four of the samples, HPC-PMMA and HPC-G1-PMMA (entries 2, 4, 12, and 14 in Table 2), were subjected to SEC analysis. The molecular weight distributions of HPC-PMMA were broad, with PDIs of 3.7 and 4.1, respectively, and showed slight bimodal characters, while the HPC-G1-PMMA samples were more narrow (PDI = 1.2 and 2.0) as depicted in Table 4. This suggests that the ATRP from HPC-G1-I shows a more controlled character than from HPC−I, possibly due to higher solubility or less crowding in the former. The polymers that were allowed to reach high conversions (entries 2 and 12 in Table 2) show that the molecular weight of HPC-G1-PMMA is much higher than that of HPC-PMMA (cf. M_w 908 500 and 308 100 g mol^{-1}, Table 4). This also suggests that the initiating efficiency was high for both initiators.

Attempts to cleave off the polymer grafts have been performed, using both alkaline and acidic media under different reaction conditions, but degradation of the polymer grafts could in all cases be observed in addition to degradation of HPC. Control degradation experiments using unmodified HPC and free PMMA, in separate reaction vessels, have been performed using similar reaction conditions. The degradation was monitored using SEC analysis before and after the degradation experiments. In all cases, degradation of the free PMMA could be observed when using milder conditions than for unmodified HPC.

The "livingness" of HPC-PMMA and HPC-G1-PMMA was explored by polymerization of a second block using *tert*-butyl acrylate as outlined in Scheme 3. By comparing the peaks in the ^{1}H NMR spectrum after polymerization (3.60 ppm: methyl groups in PMMA and 1.44 ppm: *tert*-butyl group in PtBA), the length ratio of PMMA to PtBA can be determined as 1:0.58. The reaction conditions and results for these polymerizations are displayed in Table 3 and Figure 2b.

Figure 2 shows FTIR spectra of HPC-PMMA (Figure 2a), HPC-PtBA (Figure 2b), and HPC-PAA (Figure 2c). The success of grafting a second block using *t*-BA can easily be observed; the relative intensities of the absorbances associated with sp^3 C−H stretching of methyl and methylene groups at 2947 and 2922 cm^{-1} (Figure 2b), originating from the *tert*-butyl group and the polymer backbone in PtBA, increased significantly after reaction. Since every *t*-BA unit contributes three methyl groups and one carbonyl group, it is obvious that the ratio between methyl groups and carbonyl groups will be different from that in HPC-PMMA. As seen in Figure 2a,b, the ratio of the absorbance between these peaks (2947 and 1723 cm^{-1}) has changed after grafting of *t*-BA. The carbonyl peak, at 1723 cm^{-1}, does not change frequency detectably when *t*-BA is grafted onto the PMMA block, which is expected since the acrylate carbonyl groups of PMMA and PtBA experience a similar chemical environment. The symmetric deformation mode vibration of the *tert*-butyl groups, a doublet at 1392 and 1366 cm^{-1}, is another feature of PtBA that is clearly visible in the FTIR spectrum.[37] Selective acidolysis of the *tert*-butyl groups of the PtBA block for the preparation of poly(acrylic acid) (PAA) was accomplished using trifluoroacetic acid in THF, according to an established method (Scheme 4).[38] After 24 h at ambient temperature, the remaining TFA, byproduct, and solvent were removed through evaporation at elevated temperature and reduced pressure. The resulting block copolymer showed completely different solubility properties (i.e., the solubility in THF and toluene was decreased, whereas some solubility could be observed in water). Characterization was performed using FT−IR spectroscopy (Figure 2c). The removal of the *tert*-butyl

Table 2. ATRP and Reaction Conditions of Different Monomers Initiated by the Macroinitiators

sample	[M]/[I][a]/[Cu(I)][b]/[Cu(II)][c]/[L]	monomer	initiator	toluene (wt %)	temp (°C)	time (h)	conversion (%)
1	100:0.28:0.80:0.20:1	MMA	HPC-I	50	70	48	24.8
2	100:0.28:0.80:0.20:1	MMA	HPC-I	50	80	19	39.0
3	100:0.28:0.90:0.10:1	MMA	HPC-I	50	70	21	gelled
4	100:0.14:0.80:0.20:1	MMA	HPC-I	50	70	20	10.0
5	100:0.14:0.80:0.20:1	MMA	HPC-I	50	70	19	2.9
6	100:2.50:0.90:0.10:1	HDMA	HPC-I	50	80	1	gelled
7	100:2.50:0.90:0.10:1	HDMA	HPC-I	56	70	2	gelled
8	100:2.50:0.80:0.20:1	HDMA	HPC-I	60	65	1	gelled
9	100:1.25:0.80:0.20:1	HDMA	HPC-I	67	50	1	gelled
10	100:0.19:0.80:0.20:1	HDMA	HPC-G1-I	67	50	2	18.0
11	100:0.085:0.80:0.20:1	MMA	HPC-G1-I	50	70	24	19.4
12	100:0.085:0.80:0.20:1	MMA	HPC-G1-I	50	70	20	22.8
13	100:0.085:0.90:0.10:1	MMA	HPC-G1-I	50	70	20	8.3
14	100:0.13:0.80:0.20:1	MMA	HPC-G1-I	50	70	20	14.5
15	100:0.085:0.80:0.20:1	MMA	HPC-G1-I	50	70	19	5.7

[a] [I] = mol of bromine, calculated from elemental analysis. [b] [Cu(I)Br]. [c] [Cu(II)Br_2].

Table 3. ATRP and Reaction Conditions of *tert*-BA Initiated by HPC-PMMA

sample	[M]/[I][a]/[Cu(I)][b]/[Cu(II)][c]/[L]	monomer	initiator	toluene (wt %)	temp (°C)	time (h)	conversion (%)
1	100:0.050:0.80:0.20:1	*tert*-BA	HPC-PMMA	50	70	24	1
2	100:0.100:0.80:0.20:1	*tert*-BA	HPC-PMMA	50	70	22	3.5

[a] [I] = g of HPC-*graft*-PMMA. [b] [Cu(I)Br]. [c] [Cu(II)Br_2].

Table 4. Size Characterization Data for the Comb Polymers Obtained Using SEC, DLS in Solution, and Tapping Mode AFM

sample	M_n[a] (g/mol)	M_w[a] (g/mol)	PDI[a]	D_{av}[b] (nm)	rel variance	skew	D_{av}[c] (nm)	STD
2, HPC-PMMA[d]	83 700	308 100	3.7	96[e]	0.80	1.87	91	11
4, HPC-PMMA[d]	76 500	313 700	4.1					
HPC-PMMA-PtBA[f]				280	0.07	0.52	189	20
12, HPC-G1-PMMA[d]	758 900	908 500	1.2	195	0.68	1.55	110	18
14, HPC-G1-PMMA[d]	39 100	78 000	2.0					
HPC-G1-PHDMA				183	0.14	0.95	99	16

[a] Obtained by SEC in THF, calibrated with linear polystyrene standards. [b] Number average diameter measured by DLS. [c] Average diameter measured by tapping mode AFM. [d] Sample number from Table 2. [e] Obtained in THF. Three outlying samples left out. [f] Entry 2, Table 3.

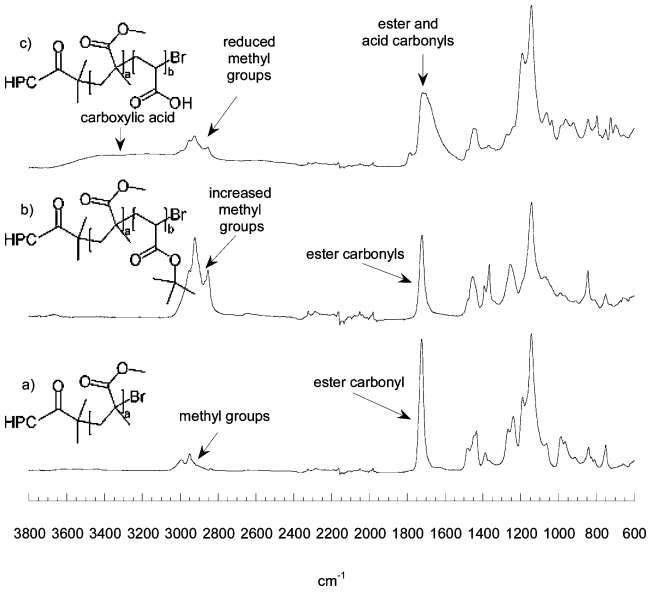

Figure 2. FTIR of (a) HPC-PMMA, (b) HPC-PMMA-PtBA, and (c) HPC-PMMA-PAA.

groups can be observed as a large decrease in the absorbance at 2947 cm^{-1} when comparing Figure 2b,c. The peaks associated with the deformation mode vibration of the *tert*-butyl groups at 1392 and 1366 cm^{-1} also disappeared after the reaction. The carbonyl absorbance of HPC-PMMA-PAA was found to be bimodal, due to a combination of the remaining ester carbonyl groups in the PMMA block at 1720 cm^{-1} and the acid carbonyl groups in the PAA block at 1702 cm^{-1}. The appearance of a broad peak, ranging from 3000 to 3700 cm^{-1}, originating from the carboxylic acid groups in the formed PAA block is further evidence of successful deprotection.

Thermal Properties. The thermal properties of the grafted polymers were characterized by DSC and TGA. The DSC traces of HPC, HPC−I, and HPC-G1-I are displayed in Figure 3.

Significant differences were observed between the DSC traces of HPC, HPC−I, and HPC-G1-I. No glass transition could be observed in the trace of HPC in the temperature range under investigation (−20−140 °C), which also has been observed by others.[39] However, HPC−I and HPC-G1-I exhibited transitions at ca. 0 and 5 °C, respectively. HPC-G1-I also showed a less pronounced transition at ca. 40 °C, which could be attributed to the glass transition of the bis-MPA unit since an earlier study on the thermal properties of dendronized bis-MPA polymers supported a T_g in that region.[4] The thermal properties of the comb polymers and the block copolymers were dependent on the type of the grafted polymer. The DSC traces of HPC-PMMA and HPC-G1-PMMA, depicted in Figure 4a, show glass transitions around 125 °C, which can be attributed to the PMMA side chains.

When a second block (of *tert*-butyl acrylate) was polymerized onto HPC-PMMA to form HPC-PMMA-PtBA, the DSC trace showed a glass transition temperature at a lower temperature, ca. 30 °C, associated with the PtBA block, as displayed in Figure

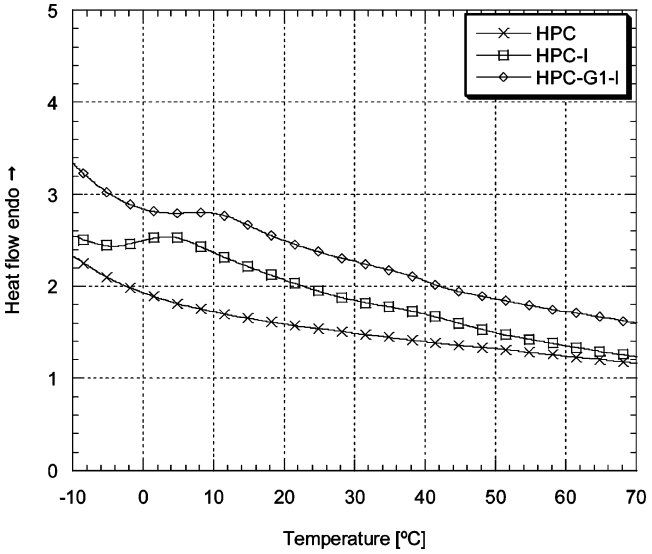

Figure 3. DSC traces of native HPC, the macroinitiator HPC-I, and the first generation dendronized macroinitiator HPC-G1-I.

4b. The transition occurs in two steps: the first showing the major step at 30 °C and the second showing a smaller step at 45 °C. Glass transition temperatures of PtBA prepared by ATRP have been reported earlier in the range of 34−46 °C.[23,38,40] However, no indication of a glass transition of the PMMA block can be observed in this thermogram. This might be due to that the blocks are not phase separated or that the flexible PtBA block greatly lowered the PMMA block T_g. The DSC trace of HPC-G1-PHDMA (Figure 4c) clearly shows a melting peak at 18 °C, which is due to the melting of the hexadecyl side chains present in PHDMA.

As seen in Figure 5, the thermal decomposition of HPC occurs by a one-step mechanism displaying the maximum degradation at 375 °C. A residue of ca. 6 wt % remains after heating HPC to 500 °C. When HPC is reacted with bromine containing compounds to form HPC−I and HPC-G1-I, the thermal stability is decreased significantly, and the mechanism no longer occurs in one step.

HPC−I underwent its first and major decomposition step at 220 °C, where ca. 70 wt % of its weight was lost. The lowered thermal stability might be a result of the introduction of the bromoalkyl units, which may eliminate HBr upon heating, catalyzing further degradation.[41] The second degradation step occurred over a wider temperature range, from 240 to 315 °C, leaving a residue of ca. 12 wt %. The thermal degradation pattern of HPC-G1-I was similar to that of HPC−I, although a third degradation step could be observed. After the initial thermolysis at 235 °C, roughly 20 wt % was lost. The second degradation step ranged from 245 to 285 °C and an ca. further 25 wt % degraded. The third step, where ca. 30 wt % was lost, had a maximum at 315 °C, leaving a residue of ca. 16 wt % when the temperature reached 500 °C. The reason for these high residual weights might be the relatively high bromine content in the macroinitiators, which also could show flame-retardant properties.[41]

The thermal stabilities of the grafted polymers were quite different from those of the macroinitiators. HPC-PMMA, whose thermogram is displayed in Figure 6a, began degrading at 225 °C but experienced a maximum mass loss at 370 °C and was not fully degraded until the temperature reached 425 °C. The degradation occurred over a wide temperature range, and the degradation pattern showed similarities to both that of HPC and that of free PMMA chains, synthesized by ATRP. However,

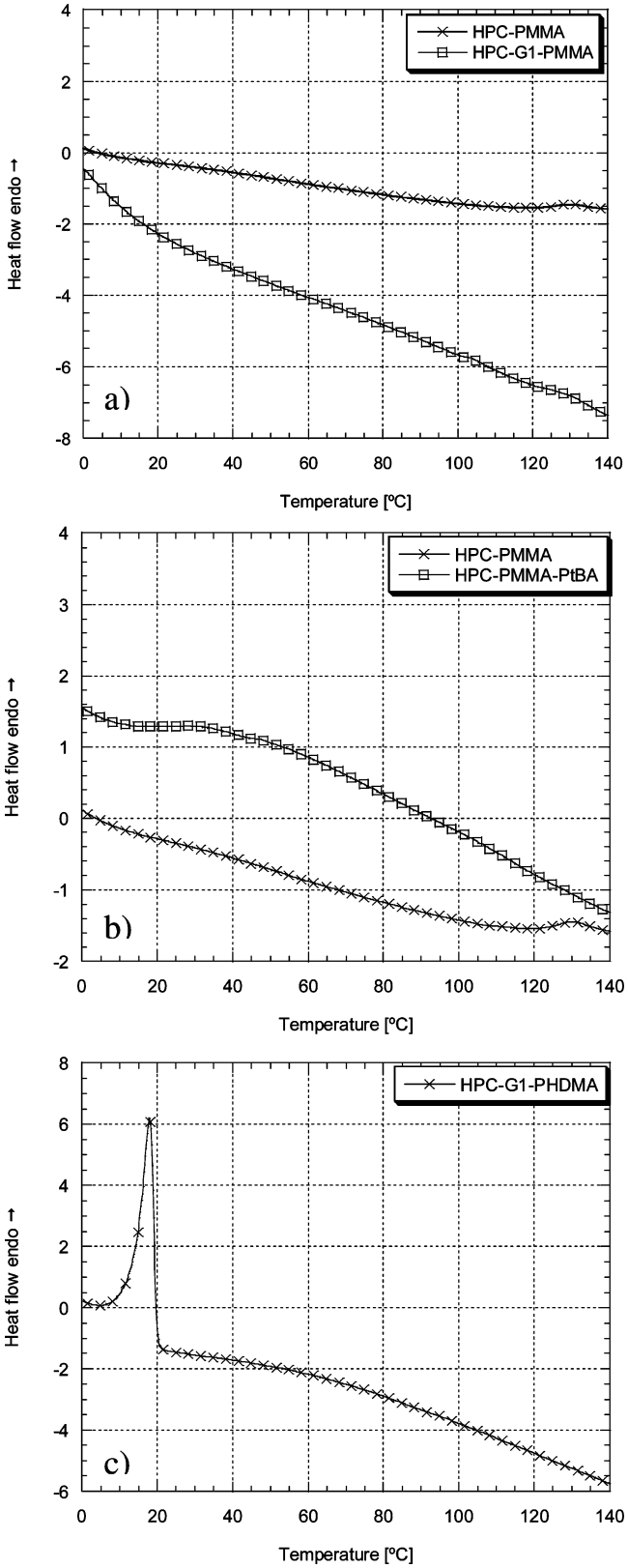

Figure 4. DSC traces of (a) HPC-PMMA and HPC-G1-PMMA, (b) HPC-PMMA and HPC-PMMA-PtBA, and (c) HPC-G1-PHDMA.

the onset of the degradation began at a lower temperature than was observed for either component, which might be due to the local high bromine content in the comb polymers.

The thermal stability of HPC-G1-PMMA was somewhat different to that of HPC-PMMA, as can be seen in Figure 6a. The onset of the degradation was at 260 °C and occurred over

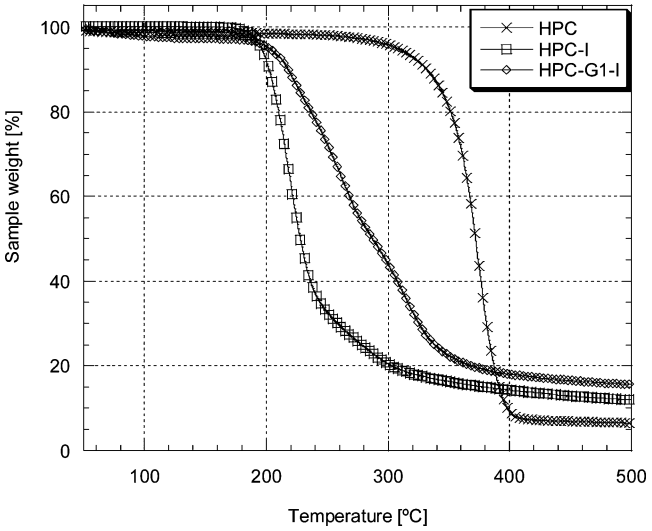

Figure 5. TGA of native HPC, the macroinitiator HPC-I, and the first generation dendronized macroinitiator HPC-G1-I.

a narrower temperature range, with the maximum degradation rate at 310 °C. At 380 °C, the degradation was complete, leaving a residue of 2.5 wt %. When *t*-BA was grafted from HPC-PMMA, the new block was clearly visible when TGA was performed. The characteristic loss of the *tert*-butyl group, which occurs up to 250 °C, is easily identified in Figure 6b. At 250−320 °C, the degradation of the PMMA and the PtBA backbone occurred simultaneously, and above these temperatures, the residual PMMA and HPC underwent degradation. The weight fraction of PtBA in HPC-PMMA-PtBA, based upon the TGA results, is estimated as 30 wt %. The thermal decomposition of HPC-G1-PHDMA, shown in Figure 6c, began at 210 °C, similar to that observed for homoPHDMA synthesized by ATRP. While the free PHDMA give an abrupt and complete degradation at 350 °C, probably associated with the degradation of the hexadecyl chains, the degradation of HPC-G1-PHDMA occurred over a broader interval, with complete degradation at 450 °C. The broadening of the degradation is most likely due to the HPC-G1 backbone.

Rheological Properties. The rheological properties of HPC-PMMA and HPC-G1-PMMA were significantly different from those of non-grafted HPC and non-grafted MMA. Master curves, with the reference temperature set to 135 °C, were created by running dynamic frequency sweeps at six temperatures for HPC, HPC-PMMA, and HPC-G1-PMMA (entries 2 and 12 in Table 2).

The complex viscosity (*Eta**) as a function of frequency for HPC (Figure 7) shows a non-Newtonian shear-thinning behavior over the entire frequency range. This behavior is representative of high molecular weight untangled molecules that can easily be oriented in the direction of flow. When PMMA was grafted from HPC, the complex viscosity increased by almost half an order of magnitude at the lowest frequencies investigated, and in this region (ca. 0.01−0.1 rad s^{-1}), both HPC-PMMA and HPC-G1-PMMA exhibited a shear-thinning behavior. HPC-PMMA and HPC-G1-PMMA displayed similar complex viscosity patterns over the entire frequency region. It is noteworthy that the dendritic-PMMA grafted material has more than twice the molecular weight as its linear analogue while still exhibiting the same viscosity. This suggests that HPC-PMMA and HPC-G1-PMMA exhibit rheological properties similar to those of conventional star polymers.[42]

The storage, G', and loss moduli, G'', of HPC-PMMA, HPC-G1-PMMA, and free PMMA synthesized through ATRP as a function of frequency are displayed in Figure 8. The storage modulus of the free PMMA is higher than that of the HPC-(G1)-PMMA grafts over the entire measured frequency region. This implies that the comb-like structure of the polymer has a softening effect on the PMMA. At high frequencies, the moduli represent the glassy state of the polymers, whereas the rapid decrease of the moduli when the frequency is lowered can be

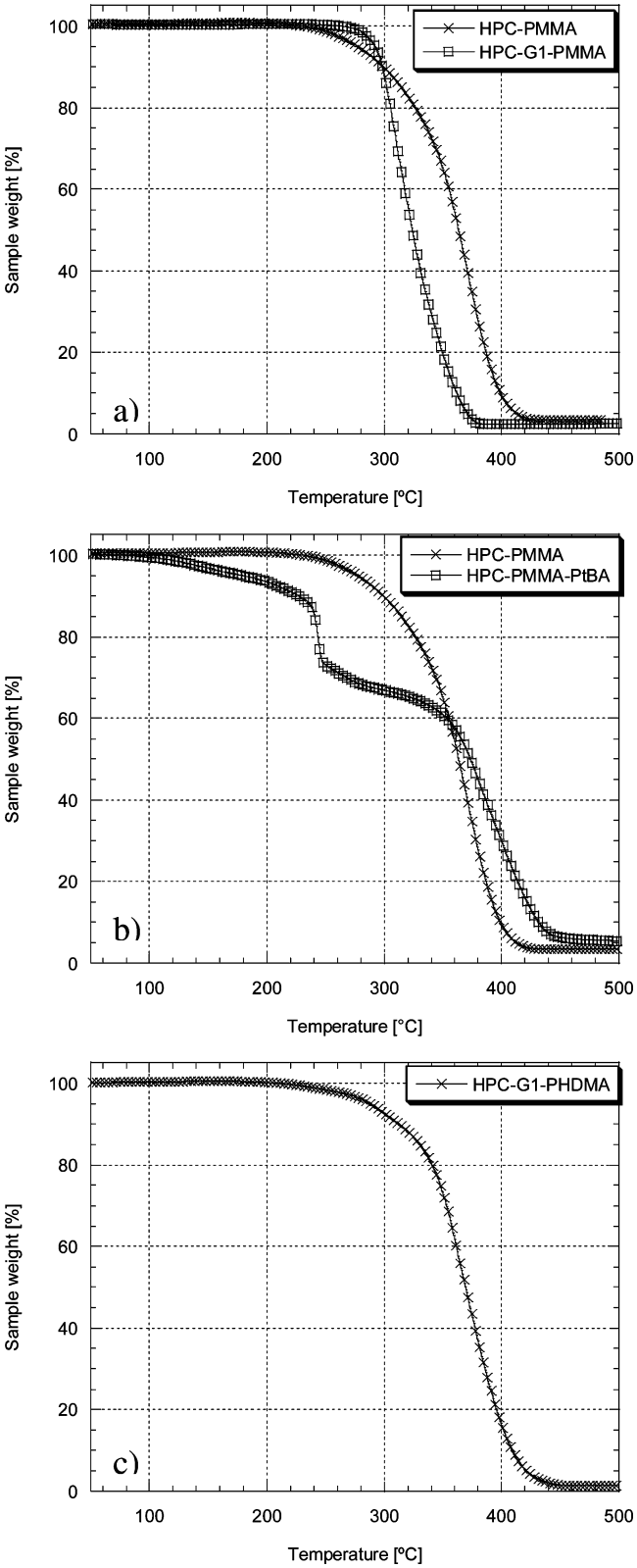

Figure 6. TGA of (a) HPC-PMMA and HPC-G1-PMMA, (b) HPC-PMMA and HPC-PMMA-PtBA, and (c) HPC-G1-PHDMA.

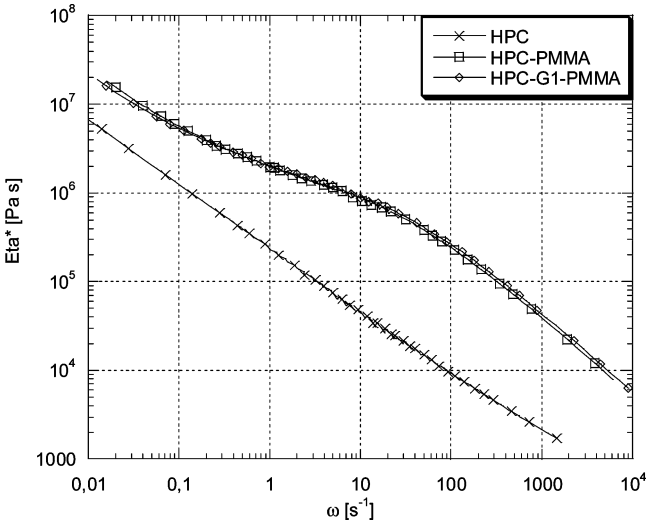

Figure 7. Complex viscosities, *Eta**, of HPC, HPC-PMMA, and HPC-G1-PMMA as a function of frequency (master curves obtained with $T_{ref} = 135$ °C).

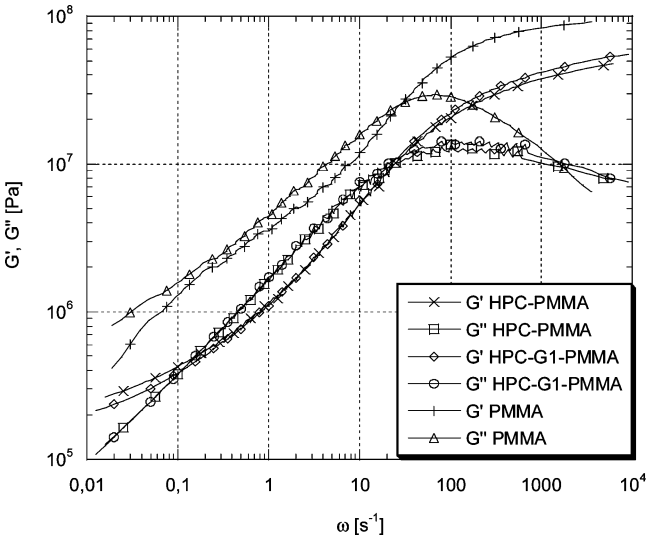

Figure 8. Frequency dependencies of shear moduli, storage *G′* and loss *G″* moduli, of HPC-PMMA, HPC-G1-PMMA, and PMMA (master curves obtained with $T_{ref} = 135$ °C).

explained by the increasing mobility of the polymers. At low frequencies, the polymers are in the frequency range where segmental mobility is possible and is therefore comparable to a polymer above its glass transition temperature. In this region, the largest differences can be observed between the PMMA grafted from HPC and free PMMA. At ca. 0.1 s^{-1}, HPC-PMMA and HPC-G1-PMMA show $G'-G''$ cross-overs, a rubber-like behavior, which is associated with chain entanglements that only exist in polymers of high molecular weight or that are lightly cross-linked.

Size Characterization. The sizes of the polymers were analyzed by DLS and tapping mode AFM. The extremely high molecular weight of the comb polymers made some of them unsuitable for characterization by SEC since avoiding fractionation of the samples during filtration and even accomplishing filtration (0.45 μm Teflon filters) were not possible in all cases.

DLS in solution was found to be a useful method for characterization of the comb polymers. Native HPC, HPC−I, and HPC-G1-I were also subjected to analysis by DLS. Different solvents, such as toluene and THF, wherein these molecules showed good solubility, were evaluated, but in each case, poorly defined aggregates were detected. However, the comb polymers that were analyzed by DLS showed good agreement with the CONTIN autocorrelation function. Their number average diameters are displayed in Table 4.

The size and shape of the grafted HPC compounds were characterized using tapping mode AFM on samples that were spin coated upon freshly cleaved mica. To avoid erroneous conclusions about the sizes of the macromolecules depending on concentration artifacts, different sample concentrations were spun cast and analyzed, ranging from 0.01 to 1.0 mg mL^{-1}. Attempts were made to study the unmodified HPC by AFM, but it was impossible to visualize single molecules of HPC using the conditions and instrument setup employed. Single molecules of HPC−I and HPC-G1-I could not be observed, although highly diluted solutions were spin coated. As for DLS analysis, HPC−I and HPC-G1-I formed molecular aggregates that by inspection were much larger than the polymer-grafted HPC.

When polymers were grafted from HPC-I, the graft copolymers could be visualized by AFM. As an example, HPC-PMMA was detected as nanometer-scale globules of uniform dimensions, with heights of approximately 5 nm (Figure 9).

The globular shape is likely due to the nature of the grafting density, the nature of the substrate, and the solution state and drying conditions used for the sample preparation.[43−46] The size averages, D_{av} in Table 4, were determined by counting the first 10 molecules from top to bottom on a representative height AFM image. As can be seen in Table 4, the sizes of the dendronized (HPC-G1) grafts were larger than those grafted directly from HPC. This is true both for data obtained using DLS and for data obtained using AFM, although in this case, the data obtained using AFM generally give lower values than the DLS analysis. This difference is expected since the polymers are in solution when DLS is performed and in the solid state during the AFM analysis, and each of the DLS fits and AFM interpretations are complicated by the molecular shapes differing from spheres.

The size of the block copolymer HPC-PMMA-PtBA was found to be larger than its precursor, HPC-PMMA, both when DLS and when AFM analyses were performed. The fraction of *tert*-BA, obtained by TGA, was 30 wt %, which implies that the size should increase when the chains are extended.

At films cast from 1.0 mg mL^{-1} solutions of HPC-G1-PHDMA, it was difficult to distinguish single molecules in the height image, whereas they could easily be observed in the phase image (Figure 10). The differences observed upon comparison of each of these imaging modalities provides for qualitative identification of differences in moduli within regions of the studied polymer.[47] However, when a concentration of 0.01 mg mL^{-1} of the same polymer was cast on mica, it is probable that single molecules could be distinguished and were found to be in the same size range as the other copolymers grafted from HPC (Figure 11).

As shown by DSC, HPC-G1-PHDMA was crystalline at subambient temperature but at ambient temperature is above its melting point. Matyjaszewski et al.[48] have shown that the crystalline side chains of block copolymers containing poly(octadecyl methacrylate) are observable in the TM-AFM phase image, being distinguishable from the softer block of poly(*n*-butyl acrylate) grafted from a PHEMA segment.

Conclusion

Hydroxypropyl cellulose (HPC) was found to be a versatile multifunctional biopolymer that was readily converted into an

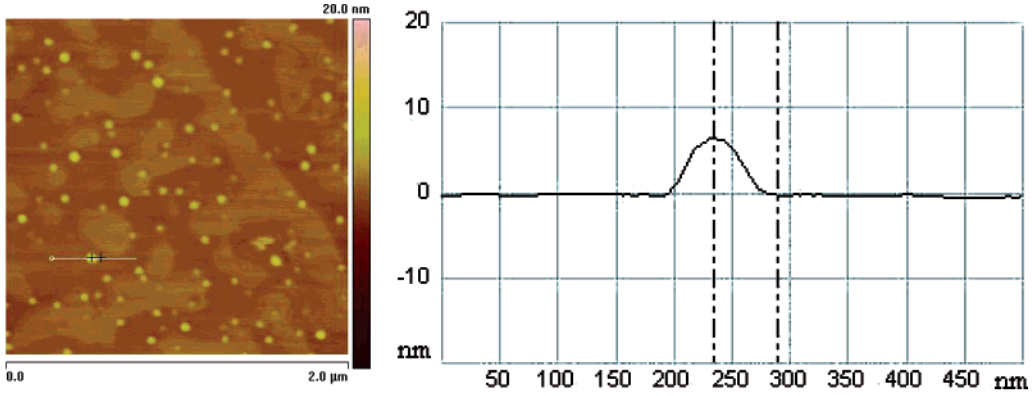

Figure 9. Height image and sectional analysis of tapping mode AFM on HPC-PMMA.

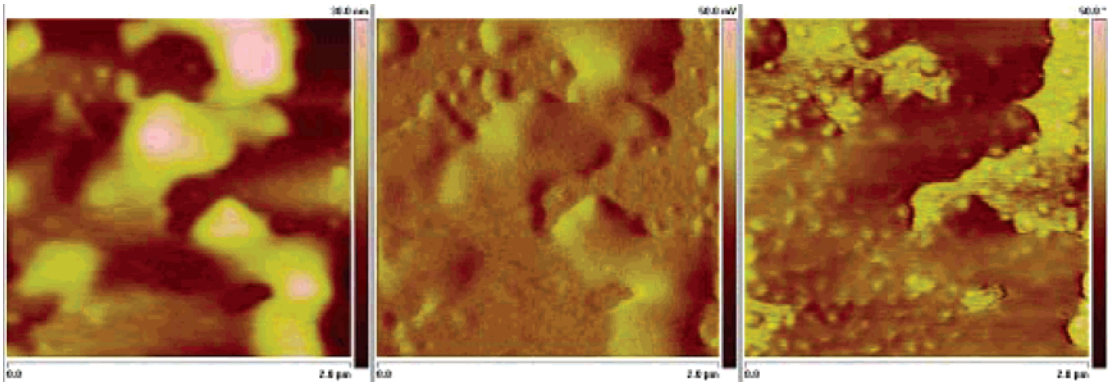

Figure 10. Height, amplitude, and phase images of tapping mode AFM on HPC-G1-PHDMA (concentration 1.0 mg mL^{-1}).

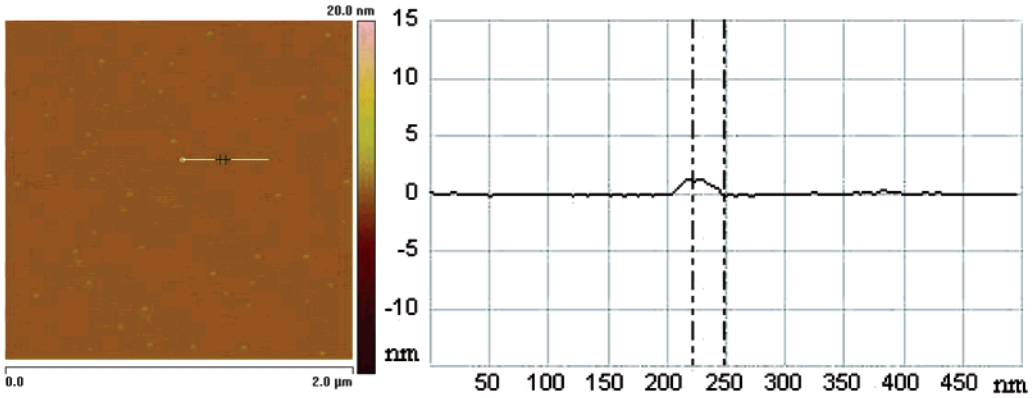

Figure 11. Height image and sectional analysis of tapping mode AFM on HPC-G1-PHDMA (concentration 0.01 mg mL^{-1}).

ATRP macroinitiator through reaction with 2-bromoisobutyryl anhydride (HPC−I). This macroinitiator was successfully used for ATRP of methyl methacrylate (HPC-PMMA). The grafting density on HPC was somewhat lowered by reacting HPC with a bis-MPA moiety functionalized with ATRP initiators (HPC-G1-I), which was then successfully utilized for ATRP of MMA (HPC-G1-PMMA).

Elemental analysis revealed that the bromine content of the macroinitiators was lower than expected. This suggests that the functionalization step, where the hydroxyl groups are reacted with ATRP initiating moieties, is difficult, as all hydroxyl groups are most likely not accessible for functionalization. The subsequent chain extension was conducted by ATRP to give comb-like polymers. The molecular weights were very high (>300 kg mol^{-1}). The polydispersity was found to be lower for HPC-G1-PMMA than for HPC-PMMA, which might indicate that the grafting process is more efficient in the former case, possibly due to a less crowded macroinitiator.

The comb−polymers were found to form discrete, spherical particles as observed by tapping mode AFM. The particle size was found to differ only slightly between the two polymers, 91 and 110 nm in diameter, respectively, which suggests that the structures are strongly collapsed in the solid phase. Molecular sizes in solution were determined by DLS and found to be more different, 96 and 195 nm, respectively, which suggests that the higher grafting affects the solubility properties, resulting in a larger hydrodynamic radius.

Both HPC-PMMA and HPC-G1-PMMA were found to be shear-thinning over the entire frequency region measured. Interestingly, their complex viscosities were very similar, despite the fact that the molecular weight of HPC-G1-PMMA is considerably higher due to the longer grafts. This suggests that HPC-PMMA and HPC-G1-PMMA exhibit rheological properties similar to those of more conventional star polymers.

HPC-PMMA was readily chain extended by *tert*-BA to give a block copolymer, HPC-PMMA-PtBA. Tapping mode AFM

Scheme 4. Deprotection of the *tert*-Butyl Groups for the Formation of Amphiphilic HPC-PMMA-PAA

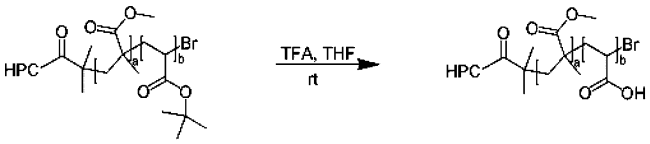

revealed discrete particles of 189 nm, significantly larger as compared to HPC-PMMA. This was also confirmed by DLS analysis, which showed a diameter of 280 nm.

An amphiphilic block copolymer was obtained through selective acidolysis of the *tert*-butyl groups to form HPC-PMMA-PAA as confirmed by FTIR and observed by the remarkable change in solubility (i.e., toluene and THF were no longer good solvents, but a slight solubility in water was observed).

A semicrystalline polymer was formed when HPC-G1-I was used to polymerize hexadecyl methacrylate (HDMA). The size of HPC-G1-PHDMA, obtained by DLS and tapping mode AFM, was 183 and 99 nm, respectively. By DSC, a melting transition, of the hexadecyl side chains, could clearly be observed at 18 °C.

Attachment of bis-MPA apparently imposed a greater control in the ATRP reaction. In our future work, we will attach larger initiator-modified dendrons to increase the grafting density. We will also explore the use of a cellulose-based backbone of even higher molecular weight to obtain cylindrical structures, functionalized with cross-linkable grafts, addressing the challenge to make tubular structures after excavation of the interior layers.[49]

Acknowledgment. This work has been financed by the Swedish Research Council Grant 2003-4210, by the National Science Foundation Grant 0301833, and by the National Institutes of Health as a Program of Excellence in Nanotechnology (HL080729).

Supporting Information Available. Calculations of the molar substitution of propoxy groups and the total degree of substitution of the initiators on HPC, NMR spectra, and chromatograms. This material is available free of charge via the Internet at http://pubs.acs.org.

References and Notes

(1) Cheng, C.-X.; Tang, R.-P.; Xi, F. *J. Polym. Sci., Part A: Polym. Chem.* **2005**, *43* (11), 2291−2297.
(2) Lee, C. C.; Grayson, S. M.; Fréchet, J. M. J. *J. Polym. Sci., Part A: Polym. Chem.* **2004**, *42* (14), 3563−3578.
(3) Nyström, A.; Hult, A. *J. Polym. Sci., Part A: Polym. Chem.* **2005**, *43* (17), 3852−3867.
(4) Nyström, A. M.; Furo, I.; Malmström, E.; Hult, A. *J. Polym. Sci., Part A: Polym. Chem.* **2005**, *43* (19), 4496−4504.
(5) Tomalia, D. A.; Kirchhoff, P. M. European Patent Application 87-101878 234408; Dow Chemical Co.: Midland, MI, 1987; p 17.
(6) Hawker, C. J.; Fréchet, J. M. J. *Polymer* **1992**, *33* (7), 1507−1511.
(7) Schlüter, A. D.; Rabe, J. P. *Angew. Chem., Int. Ed.* **2000**, *39* (5), 864−883.
(8) Carlmark, A.; Malmström, E. *J. Am. Chem. Soc.* **2002**, *124* (6), 900−901.
(9) Carlmark, A.; Malmström, E. E. *Biomacromolecules* **2003**, *4* (6), 1740−1745.
(10) Lee, S. B.; Koepsel, R. R.; Morley, S. W.; Matyjaszewski, K.; Sun, Y.; Russell, A. J. *Biomacromolecules* **2004**, *5* (3), 877−882.
(11) Coskun, M.; Temüz, M. M. *Polym. Int.* **2005**, *54* (2), 342−347.
(12) Lindqvist, J.; Malmström, E. *J. Appl. Polym. Sci.* **2006**, *100*, 4155−4162.
(13) Daly, W. H.; Evenson, T. S.; Iacono, S. T.; Jones, R. W. *Macromol. Symp.* **2001**, *174*, 155−163.
(14) Wang, C.; Dong, Y.; Tan, H. *J. Polym. Sci., Part A: Polym. Chem.* **2002**, *41*, 273−280.
(15) Shi, R.; Burt, H. M. *J. Appl. Polym. Sci.* **2003**, *89* (3), 718−727.
(16) Shen, D.; Huang, Y. *Polymer* **2004**, *45* (21), 7091−7097.
(17) Vlcek, P.; Janata, M.; Latalova, P.; Kriz, J.; Cadova, E.; Toman, L. *Polymer* **2006**, *47* (8), 2587−2595.
(18) Shen, D.; Yu, H.; Huang, Y. *J. Polym. Sci., Part A: Polym. Chem.* **2005**, *43* (18), 1099−4108.
(19) Stenzel, M. H.; Davis, T. P.; Fane, A. G. *J. Mater. Chem.* **2003**, *13* (9), 2090−2097.
(20) Hernandez-Guerrero, M.; Davis, T. P.; Barner-Kowollik, C.; Stenzel, M. H. *Eur. Polym. J.* **2005**, *41* (10), 2264−2277.
(21) Matyjaszewski, K.; Miller, P. J.; Shukla, N.; Immaraporn, B.; Gelman, A.; Luokala, B. B.; Siclovan, T. M.; Kickelbick, G.; Vallant, T.; Hoffmann, H.; Pakula, T. *Macromolecules* **1999**, *32* (26), 8716−8724.
(22) Maier, S.; Sunder, A.; Frey, H.; Mülhaupt, R. *Macromol. Rapid Commun.* **2000**, *21* (5), 226−230.
(23) Zhao, Y.; Chen, Y.; Chen, C.; Xi, F. *Polymer* **2005**, *46* (15), 5808−5819.
(24) Malkoch, M.; Carlmark, A.; Woldegiorgis, A.; Hult, A.; Malmström, E. E. *Macromolecules* **2004**, *37* (2), 322−329.
(25) Carlmark, A.; Malmström, E. E. *Macromolecules* **2004**, *37* (20), 7491−7496.
(26) Helms, B.; Liang, C. O.; Hawker, C. J.; Fréchet, J. M. J. *Macromolecules* **2005**, *38* (13), 5411−5415.
(27) Lee, C. C.; Yoshida, M.; Fréchet, J. M. J.; Dy, E. E.; Szoka, F. C. *Bioconjugate Chem.* **2005**, *16* (3), 535−541.
(28) Das, J.; Yoshida, M.; Fresco, Z. M.; Choi, T. L.; Fréchet, J. M. J.; Chakraborty, A. K. *J. Phys. Chem.* **2005**, *109* (14), 6535−6543.
(29) Yoshida, M.; Fresco, Z. M.; Ohnishi, S.; Fréchet, J. M. J. *Macromolecules* **2005**, *38* (2), 334−344.
(30) Liang, C. O.; Helms, B.; Hawker, C. J.; Fréchet, J. M. J. *Chem. Eng. Commun.* **2003**, *20*, 2524−2525.
(31) Grayson, S. M.; Fréchet, J. M. J. *Macromolecules* **2001**, *34* (19), 6542−6544.
(32) Hassan, M. L.; Moorefield, C. N.; Newkome, G. R. *Macromol. Rapid Commun.* **2004**, *25* (24), 1999−2002.
(33) Hassan, M. L.; Moorefield, C. N.; Kotta, K.; Newkome, G. R. *Polymer* **2005**, 8947−8955.
(34) Zhang, C.; Price, L. M.; Daly, W. H. *Biomacromolecules* **2006**, *7*, 139−145.
(35) Ihre, H.; Hult, A.; Söderlind, E. *J. Am. Chem. Soc.* **1996**, *118* (27), 6388−6395.
(36) Heise, A.; Nguyen, C.; Malek, R.; Hedrick, J. L.; Frank, C. W.; Miller, R. D. *Macromolecules* **2000**, *33* (7), 2346−2354.
(37) Feng, C. L.; Vancso, G. J.; Schonherr, H. *Langmuir* **2005**, *21* (6), 2356−2363.
(38) Ma, Q.; Wooley, K. L. *J. Polym. Sci., Part A: Polym. Chem.* **2000**, *38*, (S1), 4805−4820.
(39) Gómez-Carracedo, A.; Alvarez-Lorenzo, C.; Gómez-Amoza, L.; Conchiero, A. *J. Therm. Anal. Calorim.* **2003**, *73*, 587−596.
(40) Johnson, R. M.; Fraser, C. L. *Biomacromolecules* **2004**, *5* (2), 580−588.
(41) Luda, M. P.; Balabanovich, A. I.; Hornung, A.; Camino, G. *Polym. Adv. Technol.* **2003**, *14* (11−12), 741−748.
(42) Claesson, H.; Malmström, E.; Johansson, M.; Hult, A. *Polymer* **2002**, *43*, 3511−3518.
(43) Ning, F.; Jiang, M.; Mu, M.; Duan, H.; Xie, J. *J. Polym. Sci., Part A: Polym. Chem.* **2002**, *40* (9), 1253−1266.
(44) Gallyamov, M. O.; Tartsch, B.; Khokhlov, A. R.; Sheiko, S. S.; Börner, H. G.; Matyjaszewski, K.; Möller, M. *Macromol. Rapid Commun.* **2004**, *25*, 1703−1707.
(45) Gallyamov, M. O.; Tartsch, B.; Khokhlov, A. R.; Sheiko, S. S.; Börner, H. G.; Matyjaszewski, K.; Möller, M. *J. Microsc.* **2004**, *215* (3), 245−256.
(46) Gallyamov, M. O.; Tartsch, B.; Khokhlov, A. R.; Sheiko, S. S.; Börner, H. G.; Matyjaszewski, K.; Möller, M. *Chem.—Eur. J.* **2004**, *10*, 4599−4605.
(47) Wang, Y.; Song, R.; Li, Y.; Shen, J. *Surf. Sci.* **2003**, *530* (3), 136−148.
(48) Qin, S.; Matyjaszewski, K.; Xu, H.; Sheiko, S. S. *Macromolecules* **2003**, *36* (3), 605−612.
(49) Cheng, C.; Qi, K.; Khoshdel, E.; Wooley, K. L. *J. Am. Chem. Soc.* **2006**, *128* (21), 6808−6809.

BM061043W